6R.4 PRELIMINARY RESULTS FOR THE 0-1 HOUR MULTISENSOR PRECIPITATION NOWCASTER

Shucai Guan[1]*, Feng Ding[1], Richard Fulton[2], and David Kitzmiller[2]

[1]RS Information Systems, Inc.
Hydrology Laboratory, Office of Hydrologic Development
National Weather Service, NOAA, Silver Spring, Maryland

[2]Hydrology Laboratory, Office of Hydrologic Development
National Weather Service, NOAA, Silver Spring, Maryland

1. INTRODUCTION

The capability of National Weather Service (NWS) WSR-88D radar to estimate rainfall in real time makes it an attractive tool for use in NWS flash flood hydrology forecast and warning operations. Using radar rainfall data as the primary input, the Multisensor Precipitation Nowcaster (MPN) algorithm produces very short-term (0-1 hour), deterministic, regional, 4-km-gridded, precipitation forecasts (nowcasts) with computational efficiency to provide NWS Weather Forecast Offices (WFO) with additional automated forecast guidance and lead-time for issuance of flash flood warnings. These short term forecast periods are currently not well predicted by atmospheric forecast models, and thus forecasts at these short lead times depend primarily on automated extrapolation of current rainfall observations into the future. For lead times near and beyond an hour, nowcast algorithms should preferably include additional information and use more sophisticated forecasting techniques (see Wilson et al. 1998), but they come at a cost of greater computer and data requirements and associated complexity. Our goal is to implement a relatively simple rainfall nowcast system that has future expansion capability and that builds upon NWS operational rainfall estimation algorithms already existing in all our forecast offices.

In contrast to many existing nowcast algorithms that are single-radar-based, MPN integrates and mosaics data from multiple radars to provide seamless regional gridded rainfall nowcast products that alleviate known problems in estimating and nowcasting rainfall resulting from the limited scanning region of a single radar and range-related degradation of rainfall estimates due to vertical reflectivity gradients and bright bands. Even for local forecasting operations**,** forecasters can benefit from MPN by viewing multiple radars simultaneously to evaluate possible upstream features which are distant from the local radar. Current NWS plans call for implementing MPN using just the 2-3 WSR-88D radars that cover each WFO's designated area of forecast and warning responsibility, but it could be extended to much larger areas depending on the prerequisite central data collection and computer resources and defined NWS requirements for nationwide operation if necessary.

Nowcast algorithms presently used by the NWS have limited applicability to flash flood warning operations. A radar-based 0-1 h extrapolative-statistical nowcast algorithm (Kitzmiller et al., 1999) is available in AWIPS, but it produces output in probabilistic form not applicable to the automated Flash Flood Monitoring and Prediction (FFMP) system (Smith et al. 2000) A conceptually-similar 0-3 h multisensor advective-statistical forecast system which produces output for the conterminous United States twice per hour has also been in operation for several years (Kitzmiller et al. 2001). However, its forecast fields are based on a 40-km grid too coarse to permit interpretation for individual stream basins.

The purpose of this paper is to evaluate the accuracy of nowcast products from a scaled-down version of MPN and the effects of smoothing and growth/decay accounting on its performance**.** In this analysis, we extend the validation work reported in Fulton and Seo (2000) using a larger number of case studies but focus here just on single radar cases for events not experiencing range degradation and not using rain gauge data as an input data source in order to establish a baseline of performance. Future validation work will address the other important issues.

2. DESCRIPTION OF MPN

The MPN is an extension of an existing 60-minute rainfall nowcasting algorithm developed initially in the 1980's for NEXRAD implementation by the Hydrology Laboratory (HL) called the Flash Flood Potential (FFP) algorithm (Walton et al. 1985, Walton and Johnson 1986, Walton et al. 1987). Since then MPN has been enhanced and improved from both science and software perspectives and integrated together with the NWS's Multisensor Precipitation Estimator (MPE) algorithm. The MPE itself is currently operational at WFOs and River Forecast Centers. Online reference material for MPE is available at: (http://www.nws.noaa.gov/oh/hrl/papers/papers.htm#wsr88d).

The FFP algorithm was originally designed as a single-radar, single-sensor algorithm that utilizes radar-

* *Corresponding author address:* Shucai Guan, W/OHD12, 1325 East-West Highway, Silver Spring, MD, shucai.guan@noaa.gov.

derived rainfall data from the WSR-88D's Precipitation Processing System (PPS; Fulton et al. 1998) as its input out to 230 km range on the 4-km HRAP (Hydrologic Rainfall Analysis Project) grid (a polar stereographic projection), but the new MPN algorithm expands upon that paradigm with capability for multiple radar data input. And instead of using radar-only rainfall estimates from PPS, it will use rainrate estimates from the MPE algorithm that have been adjusted for possible biases using recent antecedent rain gauge data. The gauge-adjusted rainrate estimates output by MPE are input to MPN. Since much rain gauge data is available only after an operationally-significant time lag, we envision its use primarily in terms of bias adjustment rather than direct input to the multisensor analysis.

Our vision is an operational, integrated MPE/MPN rainfall analysis and nowcast package for use in flash flood monitoring and warning at the WFOs once it is integrated with the existing WFO FFMP algorithm.

The algorithm logic is described more fully in Fulton and Seo (2000), but a brief summary is provided here. Fundamentally, the most recent HRAP gridded radar rain rate field (computed using a chosen Z-R relationship) is compared with the one about 15 minutes earlier to estimate the local motion of areas of echoes on a 20 km grid scale using a standard local pattern-matching scheme.

The gridded rain rates are then projected forward in time using the most-recent estimated gridded motion vectors at a timestep small enough to prevent pixel jumping (aliasing) of the echoes (about a 3 minute timestep is necessary for the 4 km grid scale). The algorithm then computes smoothed forecasted rain rate fields by spatially smoothing them using various square spatial filters that increase in area with increasing lead time. MPN provides the user with three options for this progressive spatial smoothing of each of these forecasted rain rate fields: 1) no progressive smoothing, 2) adaptable smoothing using the FFP method, or 3) fixed smoothing using a method proposed by Bellon and Zawadski (1994) (hereafter called BZ94). They demonstrated that empirically-based progressive (increasing in area) smoothing of forecasted rain rates with increasing forecast lead time results in improved forecast performance and lower root mean square error. The BZ94 technique uses an empirically-derived, fixed relationship between smoothing area and lead time. The FFP method for smoothing (Walton et al. 1985) is conceptually similar, but it computes a variable, adaptable rate of smoothing with time that is calculated based on the current observed rain rate fields that accounts for observed changes in echo structure over the past 15 minutes. These three methods are compared for their impact on MPN's rainfall forecast performance. More sophisticated techniques that account for normally-degraded rainfall predictability with time from observation-driven nowcasts have been tested elsewhere (e.g., Seed 2003).

Additionally, MPN allows the user to choose whether local storm motion vectors (at 20 km spacing) are used or whether a single spatially mean storm motion vector is used during the forecast generation. Both methods utilize estimated storm motion vectors over the past hour to aid in computing reliable gridded vectors. In either case, the forecasted rain rate fields during the forecast period are then added up to form a one-hour rainfall forecast. This process is repeated every volume scan (every 5 or so minutes) as new radar data is received so that the one-hour forecasts are updated every 5 minutes.

Growth and decay of local rain rates can be accounted for if desired. The algorithm compares the rain rates averaged over local 20 km boxes with those computed upstream using the scan 15 minutes previously to estimate the local lagrangian growth or decay of the storms on a 20 km grid scale. This rate of rain rate change is applied linearly to the future one-hour forecast period if desired based on an input parameter setting. The simple method, however, will not create new storms if they did not already exist in the most recent scan, and there are upper limits on how high the forecasted rain rates can get.

Our aim in this study was to demonstrate the impact of the various temporal and spatial smoothing methods, select optimal smoothing methods, and define a baseline performance level in critical heavy rainfall situations. Investigation of the effects of input from multiple radars and direct application of rain gauge data is now underway.

The legacy FFP has been running at the HL in real-time 24 hours a day for over five years in evaluation and test mode, using Sterling, VA WSR-88D (KLWX) data. Likewise, the MPN and Enhanced MPE algorithms have been running in tandem in real time for several years at HL for a 5-radar test region in the mid-Atlantic area. These MPE and nowcast products are available to NWS staff for real-time examination through a internal web site.

3. ANALYSIS METHOD

In this study, we focus on validation of seven warm season events in Maryland, Virginia, and Pennsylvania. Each of the seven cases produced flash flooding documented by the NWS. The dates of the events are presented in Table 1. Because of our case selection criteria, our analyses are necessarily conditioned on the actual occurrence of a flash flood in some part of the radar umbrella. This was done because the algorithm is specifically designed for flash flood monitoring and nowcasting and performs best for convective situations where it is recognized that life and property are at an elevated risk. We are currently examining performance for all rainfall events for the mid-Atlantic region for a whole year.

We compared forecasted rain rates at arbitrary 10 minute intervals in the forecast period out to 60 minutes with those from actual observed radar-derived rain rates for those same times. We have not yet attempted to verify the forecasts against observed rain gauge data. Comparisons of one-hour forecasts vs. observed accumulations are on-going but not described here.

As introduced in the previous section, three MPN parameter setting options are tested here for their

impact on the forecasted rain rates (other less important input parameters exist within the algorithm): 1) use or non-use of storm growth/decay accounting, 2) type of progressive smoothing (none, FFP method, BZ94 method), 3) use of local vs. area-averaged storm motion vectors. Thus there are twelve possible parameter permutations that have been examined here (see the 3-letter abbreviations defined in Table 2). Additionally we also tested the typical case of persistence, in which the storms are assumed stationary, to serve as a baseline of performance. The MPN algorithm has been run for these 7 cases for all the 13 possible algorithm configurations. We desire to determine the value added, if any, by incorporating these various techniques.

Six statistics are used to evaluate and compare the accuracy of the parameter tests. They are the probability of detection (POD), the false-alarm rate (FAR), the critical success index (CSI), correlation coefficient (COR), the root mean square error (RMSE), and bias. The bias is the sum of the forecasted rain rates divided by the sum of radar-observed rain rates over the radar domain (230 km range) during the rain event. COR and RMSE are also calculated using all pixels over the radar domain during the rain event. The performance of MPN for the 60 minute forecast is discussed first, and variations of these statistics during the interim 10-60 minute forecast period are then investigated.

4. RESULTS

Table 1 lists the average conditional rain rate, percent areal echo coverage, raining duration, and number of volume scans to verify at 60 minute forecasts for each of the 7 flash flood cases. The average conditional rain rate is computed over all raining (greater than zero) HRAP pixels (nominally 4-km on a side) in the domain during a rain event. The number of possible pixels within 230 km range is 9750 in our cases. The average rain rates vary widely from 2 to 9 mm/hr. Figure 1 shows typical examples of pairs of observed and forecasted 60-minute rain rate and one-hour accumulation images for each of the seven cases. Cases 1, 2, and 3 are scattered cellular convection. In case 4, heavy rainfall occurred at the edge of the Sterling radar umbrella. Cases 5 and 6 are linear mesoscale convective systems MCS (MCS). Case 7 is a stationary convection zone over the northern Chesapeake Bay.

Table 3 is the forecast rain rate bias at 60 min. for all tests and cases. When considering averaged results for all events (see right-most column), tests NBL and NFL have the best bias (0.99), following by PRS, NBA, and NFA (1.03). All of the above 5 tests achieve excellent bias (0.99 to 1.03). Simple advection extrapolations with no smoothing and no accounting for growth/decay using a single average vector (NNA) or the local vectors (NNL) overestimate rain rate by 11%. However, tests which turn on the growth/decay option cause forecasted rain rate to increase to 63-84% over the observed rain rates. Clearly the implemented growth/decay method adds no value to the forecasts, much as Wilson et al. (1998) and others have concluded.

Choice of smoothing options can also impact the bias. Using local vectors has a small advantage over using a single average vector when averaged over these case studies, though there are some exceptions on a case-by-case basis. For example, the two simple advection extrapolations (NNL and NNA) are the top 2 performers for case 3 while persistence gives the best performance for cases 5 and 7.

Root mean square errors (RMSE) of 60 minute forecasted rain rates for all tests and cases are shown in Table 4. Test NBL achieves again the best performance for all cases. It reduces RMSE by 22.7% on average compared to the best performance of the two simple advection extrapolations and persistence. The smoothing option in MPN has a crucial role in reducing RMSE. Employing smoothing using either the FFP or BZ94 methods decreases RMSE for 60 minute forecasted rain rates at least 17% for our cases. In general, turning off growth/decay option, using local vectors, and BZ94 smoothing scheme improve performance in RMSE.

Table 5 shows the correlation coefficients of 60 minute forecasted rain rates for all tests and cases. Test NBL has again the highest correlation for all cases although the advantage is small compared to several other test configurations. As in RMSE, the smoothing has the most impact on increasing correlation. Using local vectors can improve it as well. The effect of turning on growth/decay is mixed, but it increases correlation for most cases. Persistence has the lowest correlation for all cases.

As pointed by Wilson et al. (1998), evaluation and comparison of the accuracy of nowcasts is very difficult. Statistics such as POD and FAR do not always adequately represent performance. For example, no credit is given for correctly forecasting a nonevent or slightly missing a forecast in either time or space. However, these statistics are useful for comparing performance of parameter options in MPN since they are evaluated precisely in the same manner.

Average POD, FAR, and CSI for forecasted rain rates > 5 mm/hr at 60 minute are presented in Table 6. They are averaged over 7 flash flood cases. Turning on growth/decay option increases POD for all cases (not shown). Smoothing generally improves POD. Using local vector or average vector motion has an minor effect on POD. However, turning on growth/decay option also results in higher FAR. The range of average FAR is only from 0.69 to 0.79. It is the general tendency that smoothing and using local vector motion decreases FAR. CSI also has a narrow range from 0.16 to 0.21 for 12 tests (persistence test has a much lower CSI at 0.12). It is difficult to analyze the effect of the parameter options in MPN on CSI . However, the inclination is that smoothing and using local vector motion improves CSI and that growth/decay option has small minor effects on CSI. Test persistence, on average, possesses the worst performance with the lowest POD and CSI as well as the highest FAR. Test NBL gives the best performance

on FAR and CSI, though the gain is negligible compared to several other test configurations.

Fig. 2 shows the forecast lead time variations of the above six statistics for 4 test configurations: NNL, NFL, GNL, GFL. The statistics are averages over 7 flash flood cases listed in Table 1. The effects of the growth/decay option can be found by comparing tests NNL with GNL, or NFL with GFL. The differences between tests NNL and NFL, or between GNL and GFL are due to the beneficial influence of progressive spatial smoothing during the forecast period. The growth/decay option overestimates rain rate bias significantly, and the smoothing option improves the bias during the 60 minute forecast period (Fig.2a). The smoothing reduces RMSE substantially during the forecast period, and turning off growth/decay option results a perceptible improvement on RMSE after the 30 minute forecast (Fig. 2b). The correlations for two tests with smoothing are about the same and are higher than those without smoothing (Fig. 2c). The smoothing option increases correlation

Turning off the growth/decay option has negligible improvement on correlation. POD in Fig. 2d clearly illustrates that turning on the growth/decay option and smoothing option improve POD. As forecast lead time increases, the influence of the growth/decay option is magnified. The effect of the growth/decay option is much larger than that of the smoothing option at 60 minutes into the forecast. However, turning on the growth/decay option increases FAR, and two tests using the growth/decay option result in higher FAR during 60 minute forecasts (Fig. 2e). The smoothing produces notable improvement on FAR after the 30 minute forecast. The difference in CSI in Fig. 2f among the 4 tests is very small. It is clear that the smoothing improves CSI. The growth/decay option has small mixed effect on CSI. It improves CSI a little if comparing test NNL with GNL and reduces CSI if comparing NFL with GFL. In summary, test NFL has the best performance among the 4 tests for five of six statistics during the 0-60 minute forecast period. POD is the only exception in which NFL is second best during the 0-30 minute period and third best during the 40-60 minute period. This is understandable since tests with the growth/decay overestimate rain rate significantly and thus produce higher POD.

5. CONCLUSIONS

The performance of MPN has been investigated based on seven flash flood cases in the MD-VA-PA region. In particular, the effects of smoothing, growth/decay, and storm motion vectors on MPN performance have been examined. Our studies show that MPN produces very good 0-60 minute rain rate forecasts. MPN substantially improves all six statistics relative to the simple advection extrapolation (NNA and NNL) and persistence methods. MPN reduces RMSE by 22.7% compared to the two simple advection extrapolations or persistence. The smoothing creates major improvement for all six statistics we examined, in agreement with Bellon and Zawadski (1994). The growth/decay of rain storms is a very complicated process. More physical mechanisms should be considered beyond the simple method tested here, though achieving routine and significant success is challenging even for more advanced physically-based techniques such as NCAR's AutoNowcaster (Mueller et al. 2003). Results from our simple approach in MPN indicate that the growth/decay option has mixed effects that are not particularly positive. Using local vectors has small but noticeable improvement over single average vectors, though improvements for individual storms in individual case studies is expected to be higher if focusing just on those rare but high-impact events.

The study cases included here feature instances of various common flash-flood scenarios, such as slow-moving MCS's, multiple convection cells, and quasi-stationary convergence lines. Therefore it is likely that these results would be duplicated in forecasts for most critical rainfall situations over much of the United States. The results obtained here will be applied toward defining default parameters for the operational version of MPN, though in some locations the parameters may be modified by local users.

ACKNOWLEDGEMENTS

This work was supported by the National Weather Service's Advanced Hydrologic Prediction Services (AHPS) program.

REFERENCES

Bellon, A., and I. Zawadzki, 1994: Forecasting of hourly accumulations of precipitation by optimal extrapolation of radar maps. *J. Hydrol*., 157, 211-233.

Fulton, R. A., J. P. Breidenbach, D. J. Seo, D. A. Miller, and T. O'Bannon, 1998: The WSR-88D rainfall Algorithm. *Wea. Forecasting*, 13, 377-395.

_____ and D. J. Seo, 2000: A prototype operational 0-1 hour radar-based flash flood potential algorithm. *Preprints: 15th Conf. on Hydrology*, Long Beach, 226-228.

Kitzmiller, D. H., M. E. Churma, and M. T. Filiaggi, 1999: The AWIPS 0-1 hour rainfall forecast algorithm. *Preprints 15th International Conference on Interactive Information and Processing Systems,* Dallas, Amer. Meteor. Soc., 175-178.

_____, S. D. Vibert, and F. G. Samplatsky, 2001: Short-range forecasts of rainfall amount from an extrapolative-statistical technique utilizing multiple remote sensor observations. *Preprints Symposium on Precipitation Extremes*, Albuquerque, Amer. Meteor. Soc., 266-270.

Mueller, C, T. Saxen, R. Roberts, J. Wilson, T. Betancourt, S. Dettling, N. Oien, and J. Yee, 2003: NCAR Auto-Nowcast System. *Wea. Forecasting*, 18, 545-561.

Seed. A., 2003: A dynamic and spatial scaling approach to advection forecasting. *J. Applied Meteor*., 42, 381-388.

Smith, S. B., M. T. Filiaggi, M. Churma, J. Roe, M. Glaudemans, R. Erb, and L. Xin, 2000: Flash Flood Monitoring and Prediction in AWIPS 5 and beyond. *Preprints 15th Conference on Hydrology*, Amer. Meteor. Soc., Long Beach, 229-232.

Walton, M., E. Johnson, P. Ahnert, and M. Hudlow, 1985: Proposed on-site Flash-Flood Potential system for NEXRAD. *Preprints, 6th Conf. Hydrometeorology*, Amer. Meteor. Soc., 122-129.

_____ and _____, 1986: An improved precipitation projection procedure for the NEXRAD Flash-Flood Potential system. *Preprints, 23rd Conf. Radar Meteorology*, Amer. Meteor. Soc., JP62-JP65.

_____, _____, and R. Shedd, 1987: Validation of the on-site Flash Flood Potential system for NEXRAD. *Preprints, 21st Intl. Symp. Remote Sensing of Environment*, Ann Arbor, MI, 381-392.

Wilson, J. W., N. A. Crook, C. K. Mueller, J. Sun, and M. Dixon, 1998: Nowcasting thunderstorms: A status report. *Bull. Amer. Meteor. Soc.,* 79, 2079-2099.

Table 1. Date, average conditional rain rate (mm/h) from radar observations, average raining area coverage, raining duration (hour), and number of volume scans to verify at 60 minute forecasts for 7 flash flood cases.

Case	**1**	**2**	**3**	**4**	**5**	**6**	**7**
Date	27 Jun 95	18 Jun 96	14 Jul 00	11 Sep 00	22 Jun 01	13 Jun 03	15 Sep 03
Avg rain rate	3.07	2.64	8.83	1.95	5.89	3.69	3.33
Coverage(%)	17.6	24.3	24.7	3.9	9.1	18.1	11.4
Duration(hr)	8.1	16.0	15.5	13.6	18.8	9.1	22.2
No. of scans	75	156	161	124	175	101	208

Table 2. Test names and their input parameters.

Growth/decay	No	No	No	No	No	No	No	Yes	Yes	Yes	Yes	Yes	Yes
Smoothing	No	No	No	FFP	FFP	BZ94	BZ94	No	No	FFP	FFP	BZ94	BZ94
Motion	No	Avg	Loc	Avg	Loc	Avg	Loc	Avg	Loc	Avg	Loc	Avg	Loc
Test name	PRS	NNA	NNL	NFA	NFL	NBA	NBL	YNA	YNL	YFA	YFL	YBA	YBL

Table 3. Forecast rain rate bias at 60 minute. The bias is ∑(forecasted rain rate)/ ∑(observed rain rate).

Case	**1**	**2**	**3**	**4**	**5**	**6**	**7**	**Avg**
PRS	1.08	0.99	0.89	1.28	1.00	0.95	1.00	1.03
NNA	1.12	1.07	0.93	1.41	1.10	1.07	1.04	1.11
NNL	1.11	1.05	0.94	1.49	1.10	1.06	1.05	1.11
NFA	1.07	1.01	0.89	1.27	1.01	0.97	0.97	1.03
NFL	1.02	0.96	0.87	1.24	0.96	0.93	0.95	0.99
NBA	1.07	1.01	0.89	1.28	1.01	0.97	0.98	1.03
NBL	1.02	0.97	0.87	1.24	0.96	0.92	0.96	0.99
GNA	1.58	1.65	1.52	2.53	2.05	1.92	1.67	1.84
GNL	1.56	1.63	1.52	2.54	2.04	1.89	1.68	1.84
GFA	1.47	1.53	1.44	2.32	1.89	1.76	1.54	1.71
GFL	1.43	1.49	1.42	2.28	1.83	1.71	1.53	1.67
GBA	1.42	1.51	1.41	2.26	1.84	1.71	1.51	1.67
GBL	1.38	1.47	1.39	2.19	1.78	1.66	1.50	1.63

Table 4. Root mean square error (mm/h) for 60 minute forecasted rain rate.

Case	**1**	**2**	**3**	**4**	**5**	**6**	**7**	**Avg**
PRS	5.94	4.03	11.49	1.55	5.80	5.21	3.22	5.32
NNA	5.91	3.87	10.94	1.54	5.72	5.00	3.13	5.16
NNL	5.64	3.78	10.53	1.54	5.63	4.93	3.07	5.02
NFA	4.81	3.01	9.08	1.17	4.51	3.97	2.47	4.15
NFL	4.62	2.94	8.73	1.14	4.43	3.92	2.42	4.03
NBA	4.57	2.88	8.59	1.09	4.31	3.80	2.39	3.95
NBL	4.49	2.84	8.35	1.07	4.27	3.77	2.36	3.88
GNA	5.94	4.05	11.41	1.75	6.07	5.31	3.28	5.40
GNL	5.67	3.97	11.08	1.71	5.97	5.25	3.23	5.27
GFA	4.87	3.26	9.84	1.43	4.99	4.34	2.65	4.48
GFL	4.68	3.17	9.52	1.38	4.88	4.28	2.62	4.36
GBA	4.66	3.13	9.40	1.36	4.80	4.17	2.58	4.30
GBL	4.57	3.07	9.16	1.32	4.72	4.12	2.56	4.22

Table 5. The correlation coefficients for 60 minute forecast rain rates.

Case	1	2	3	4	5	6	7	Avg
PRS	0.30	0.15	0.16	0.13	0.11	0.05	0.24	0.16
NNA	0.31	0.23	0.24	0.13	0.15	0.14	0.29	0.21
NNL	0.36	0.25	0.29	0.16	0.17	0.15	0.32	0.24
NFA	0.38	0.35	0.33	0.19	0.24	0.22	0.41	0.30
NFL	0.43	0.37	0.38	0.22	0.26	0.23	0.43	0.33
NBA	0.41	0.37	0.37	0.21	0.26	0.25	0.42	0.33
NBL	0.44	0.39	0.41	0.23	0.28	0.26	0.44	0.35
GNA	0.33	0.28	0.31	0.15	0.21	0.20	0.34	0.26
GNL	0.38	0.30	0.34	0.19	0.23	0.21	0.36	0.29
GFA	0.40	0.36	0.36	0.18	0.27	0.27	0.41	0.32
GFL	0.44	0.38	0.40	0.20	0.28	0.28	0.43	0.34
GBA	0.40	0.37	0.38	0.17	0.27	0.28	0.41	0.32
GBL	0.42	0.38	0.41	0.19	0.28	0.28	0.42	0.34

Table 6. Average POD, FAR, and CSI of rain rate > 5 mm/h at 60 minute forecast. These statistics are averaged over the 7 flash flood cases listed in Table 1.

Test	POD	FAR	CSI
PRS	0.21	0.79	0.12
NNA	0.28	0.74	0.16
NNL	0.29	0.73	0.17
NFA	0.36	0.71	0.19
NFL	0.36	0.70	0.20
NBA	0.37	0.71	0.20
NBL	0.37	0.69	0.21
GNA	0.43	0.78	0.17
GNL	0.44	0.77	0.18
GFA	0.47	0.77	0.19
GFL	0.48	0.76	0.19
GBA	0.48	0.77	0.19
GBL	0.48	0.76	0.19

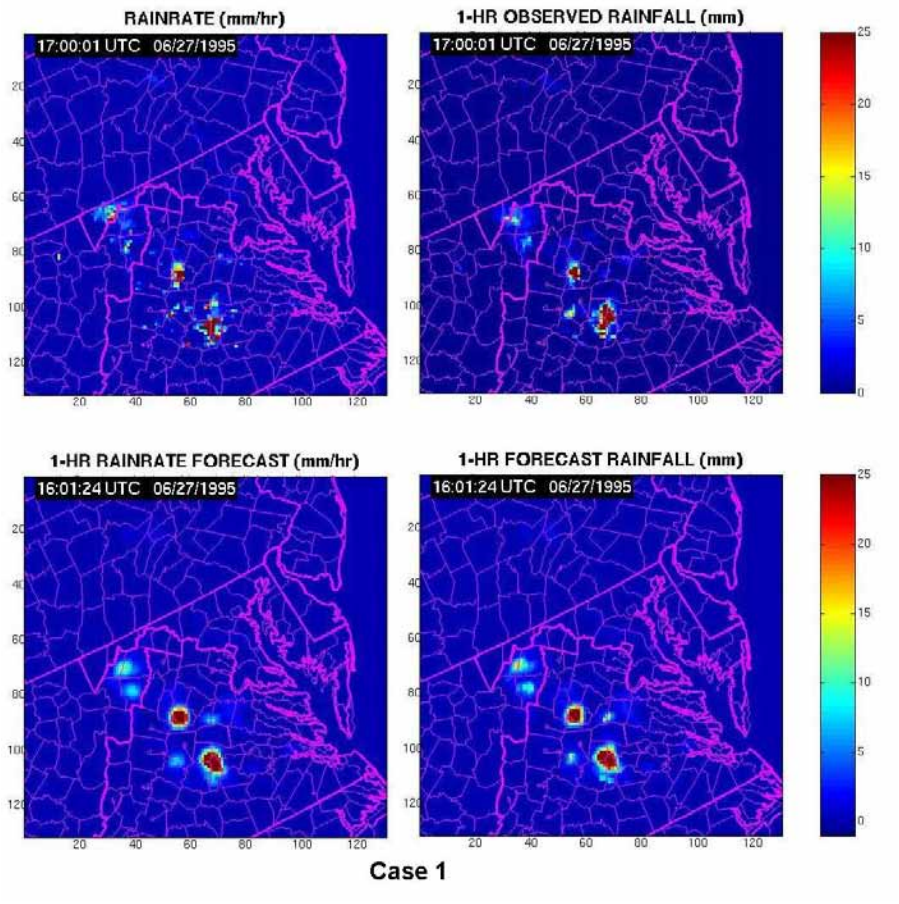
RAINRATE (mm/hr)
17:00:01 UTC 06/27/1995
1-HR OBSERVED RAINFALL (mm)
17:00:01 UTC 06/27/1995
1-HR RAINRATE FORECAST (mm/hr)
16:01:24 UTC 06/27/1995
1-HR FORECAST RAINFALL (mm)
16:01:24 UTC 06/27/1995
Case 1

(a)

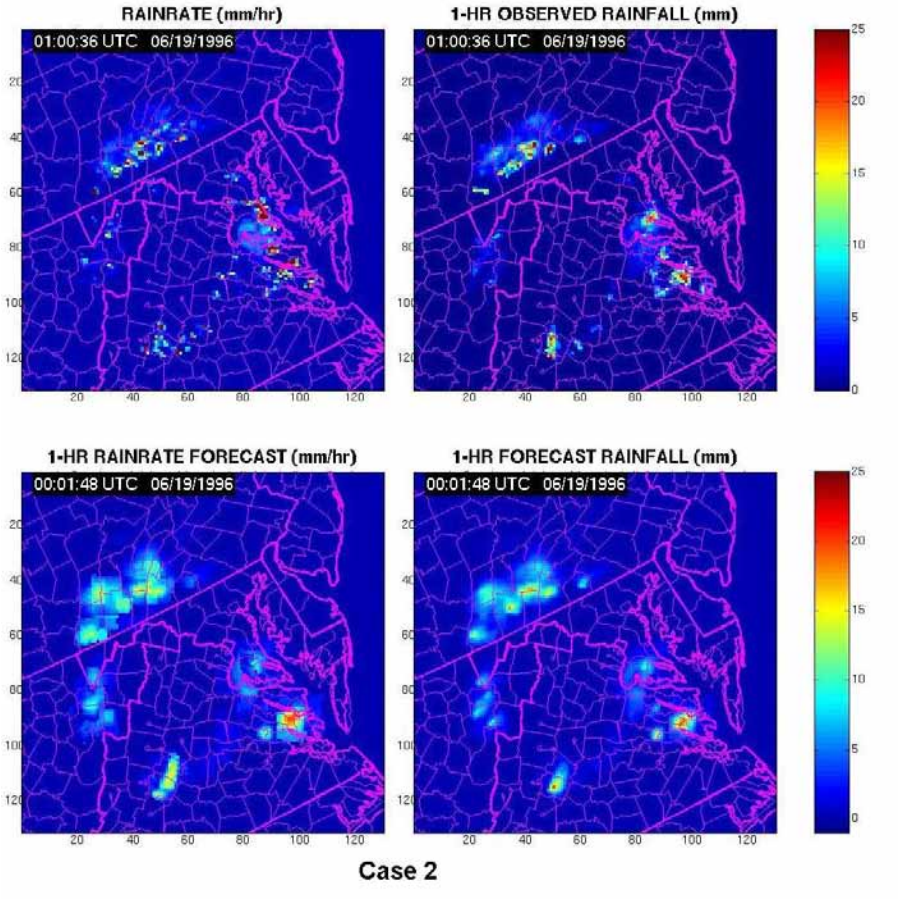
RAINRATE (mm/hr)
01:00:36 UTC 06/19/1996
1-HR OBSERVED RAINFALL (mm)
01:00:36 UTC 06/19/1996
1-HR RAINRATE FORECAST (mm/hr)
00:01:48 UTC 06/19/1996
1-HR FORECAST RAINFALL (mm)
00:01:48 UTC 06/19/1996
Case 2

(b)

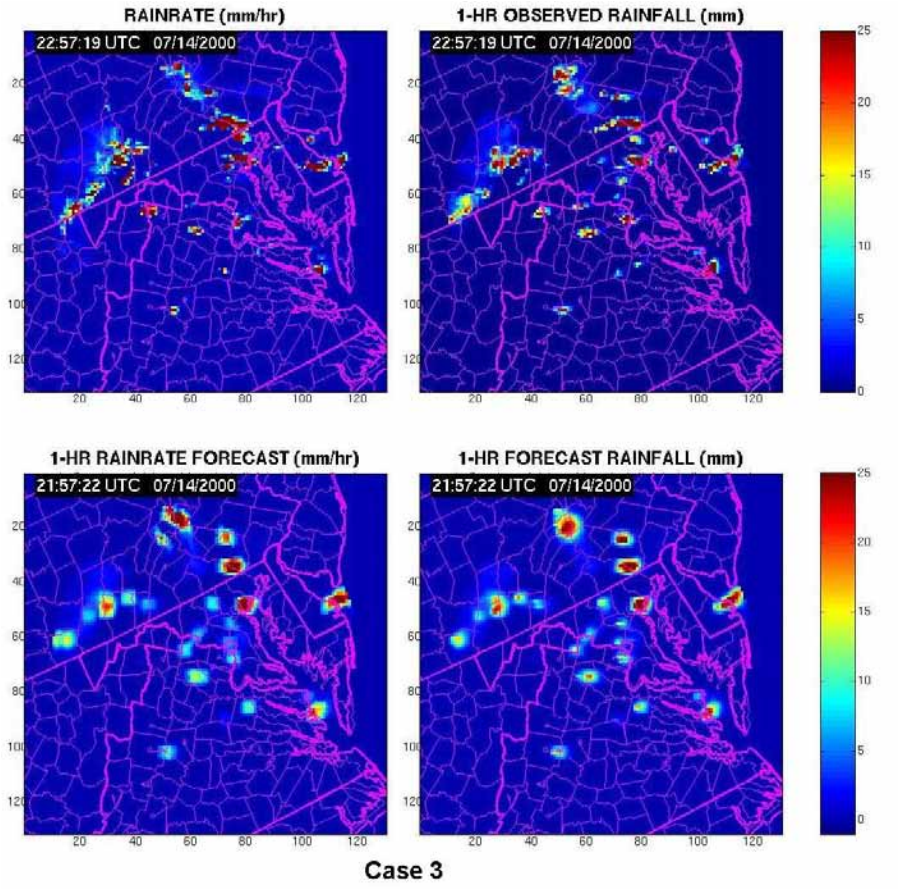

(c)

Case 3

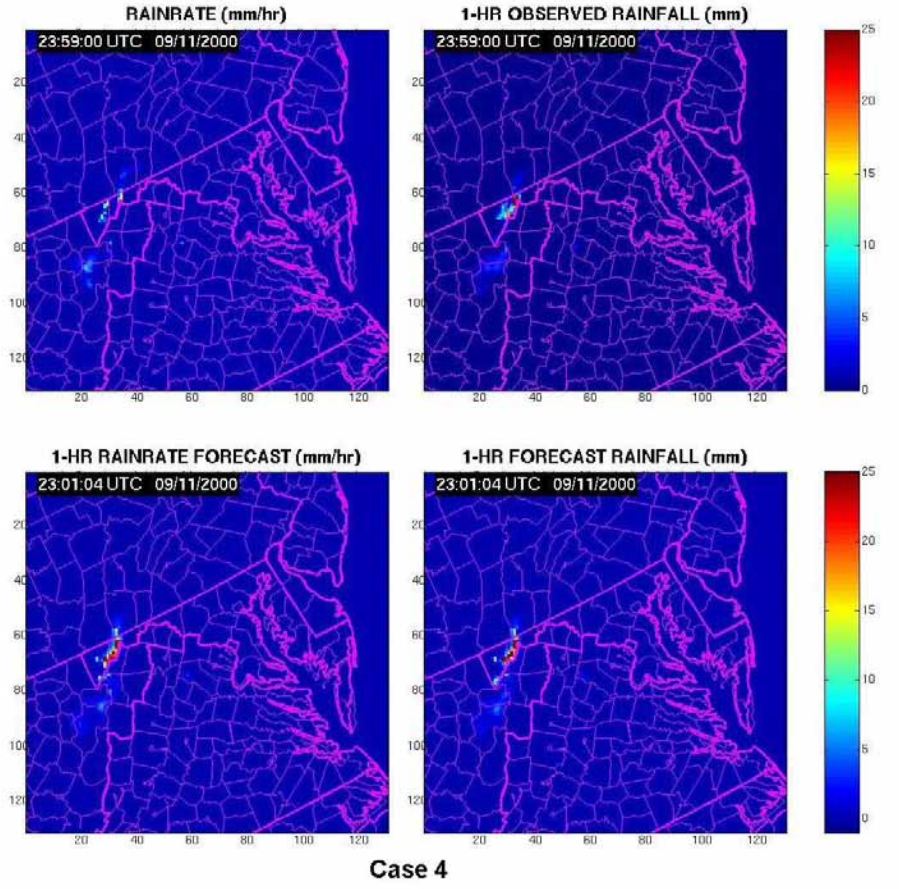

(d)

Case 4

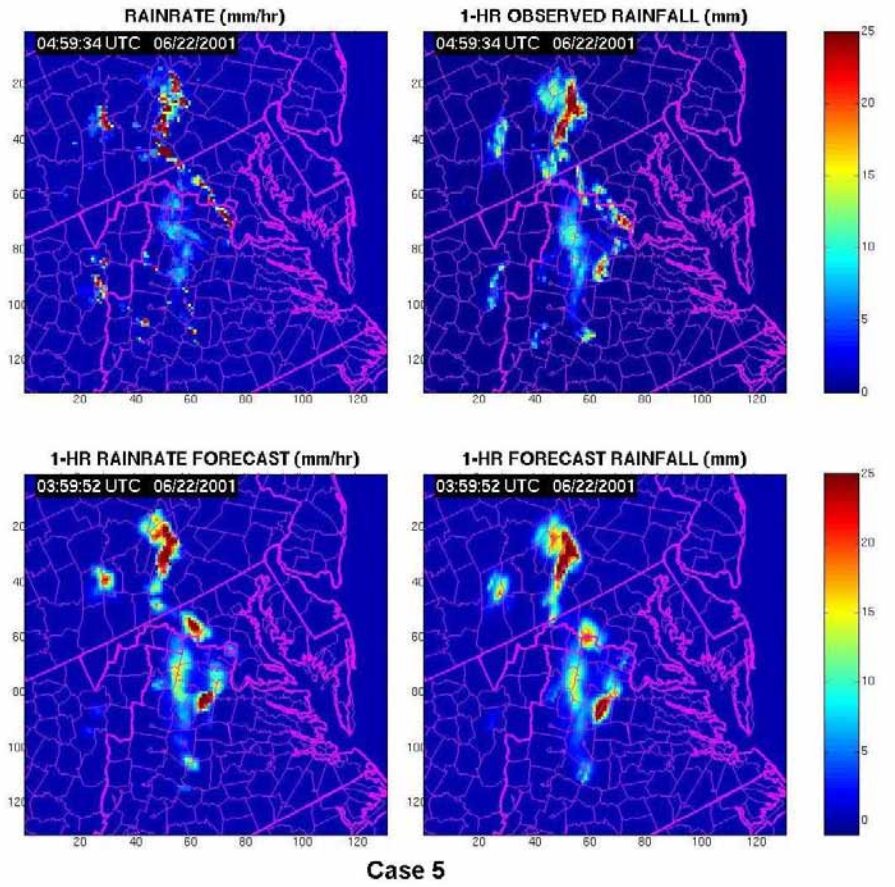

(e)

Case 5

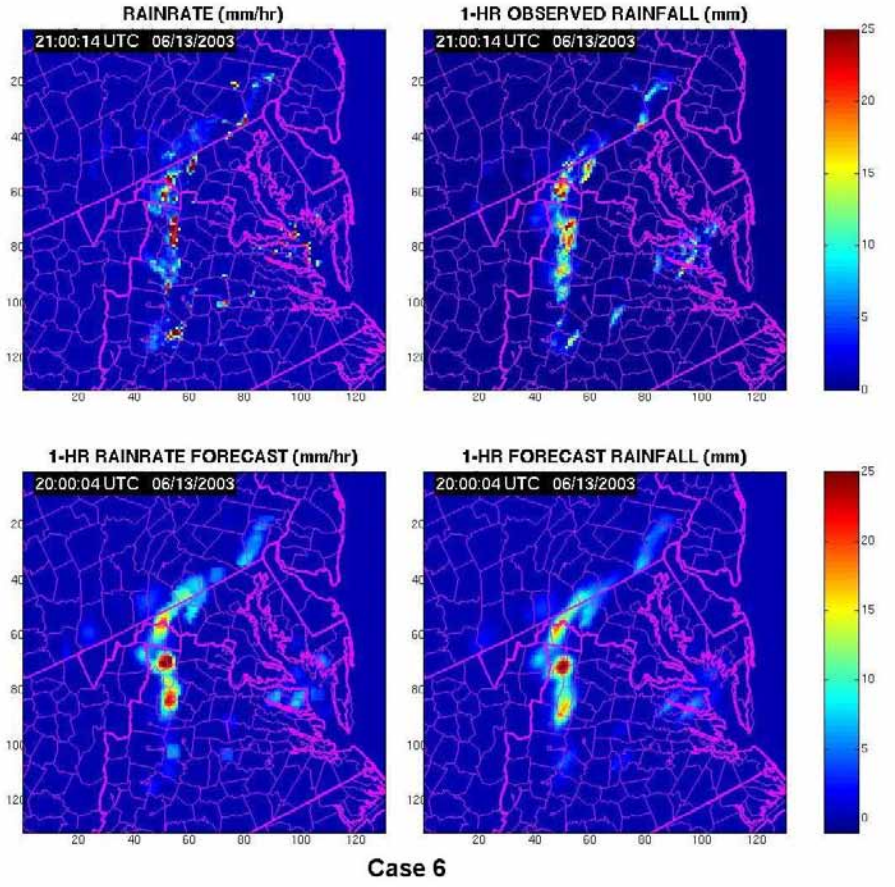

(f)

Case 6

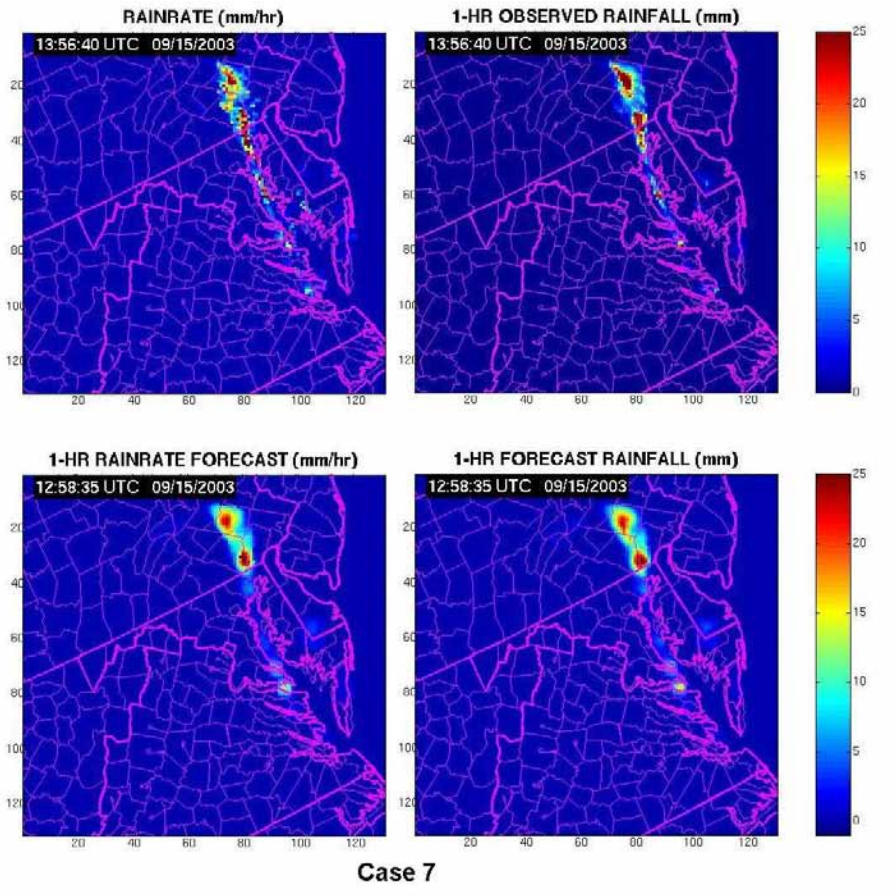

(g)

Figure 1. Examples of pairs of observed and forecasted 60-minute rain rate and one-hour accumulation images for each of the seven test cases. Subfigures (a-g) correspond to cases 1-7, respectively. All forecasts are from test option NFL.

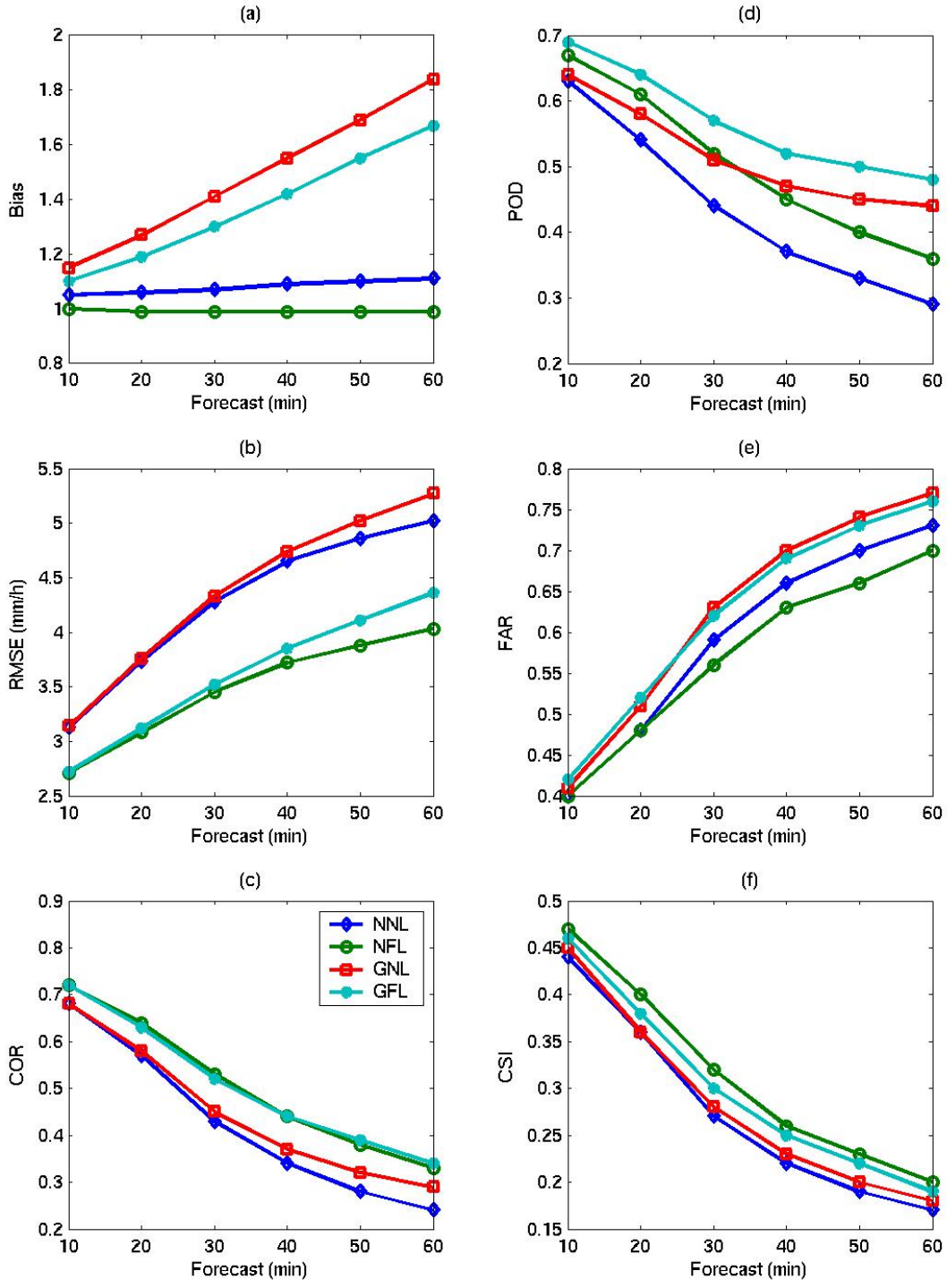

Figure 2. Forecast scores as a function of forecast lead time for 4 test configurations for all 7 rain events: (a) Bias, (b) RMSE, (c) COR, (d) POD, (e) FAR, and (f) CSI.